

# The Relation Between Optical Extinction and Hydrogen Column Density in the Galaxy

Tolga Güver and Feryal Özel

*University of Arizona, Department of Astronomy, 933 N. Cherry Ave., Tucson, AZ, 85721*

## ABSTRACT

A linear relation between the hydrogen column density ( $N_{\text{H}}$ ) and optical extinction ( $A_{\text{V}}$ ) in the Galaxy has long been observed. A number of studies found differing results in the slope of this relation. Here, we utilize the data on 22 supernova remnants that have been observed with the latest generation X-ray observatories and for which optical extinction and/or reddening measurements have been performed and find  $N_{\text{H}}(\text{cm}^{-2}) = (2.21 \pm 0.09) \times 10^{21} A_{\text{V}}(\text{mag})$ . We compare our result with the previous studies and assess any systematic uncertainties that may affect these results.

**Key words:** interstellar matter

## 1 INTRODUCTION

Photoelectric absorption by interstellar matter causes rapid attenuation of the observed soft X-ray spectra in all Galactic sources. Measuring the amount of the X-ray extinction yields information on the total column density of the interstellar matter between the observer and the source, because any element that is not fully ionized contributes to the extinction of X-rays. Although the amount of the X-ray extinction is generally expressed in terms of the equivalent hydrogen column density ( $N_{\text{H}}$ ), it is generally caused, especially above  $\sim 0.25$  keV, by the most abundant heavier elements like O, Ne, Fe, Mg, and Si.

Optical extinction, on the other hand, is caused by grains composed of these same heavier elements. Therefore, the relation between optical and X-ray extinction depends on the relative abundances of metals and the temperature of the intervening medium, which primarily determine the relative fraction of metals in grains versus in the gas state. For sources, however, that lie at large distances from the observer, photons traverse many different regions of the interstellar medium (ISM), and, thus, sample a wide variety of physical conditions. Under the assumption that different lines of sight sample the same distribution of physical conditions in the ISM, one expects a relation between the optical extinction and the hydrogen column density towards distant sources.

The relation between optical extinction and hydrogen column density has been observationally studied for decades using various techniques (see, e.g., Reina & Tarengchi 1973; Gorenstein 1975; Predehl & Schmitt 1995). Using measurements for two X-ray binaries together with the two extended sources GCX and Cas A (SNR G111.7–02.1), Reina & Tarengchi (1973) derived the first relation  $N_{\text{H}}(\text{cm}^{-2}) = 1.85 \times 10^{21} A_{\text{V}}(\text{mag})$ . Gorenstein (1975)

found a similar relation shortly afterwards using independent optical extinction and column density measurements for 7 supernova remnants (SNR), which yielded  $N_{\text{H}}(\text{cm}^{-2}) = (2.22 \pm 0.14) \times 10^{21} A_{\text{V}}(\text{mag})$ . Later, using ROSAT observations of 25 bright X-ray point sources as well as of 4 SNRs, Predehl & Schmitt (1995) determined the shape and intensity of the soft X-ray halos around these sources, which they used in conjunction with dust halo models to measure the dust column density. In this study, they also found a relation between the X-ray derived hydrogen column density and optical extinction given by  $N_{\text{H}}(\text{cm}^{-2}) = (1.79 \pm 0.03) \times 10^{21} A_{\text{V}}$ .

The three analyses quoted above resulted in relations that disagree within their statistical uncertainties. This can be a result of (i) the low quality of early X-ray spectroscopic data used; (ii) the systematic uncertainties between the methods employed, (iii) formal uncertainties because of the small number of sources used, or (iv) strong variations in the ISM along the various lines of sight. In this paper, we take advantage of the most recent X-ray and optical observations of SNRs with high quality instruments and compile the most complete set of extinction measurements towards these sources to redetermine the relation between the optical extinction and the hydrogen column density. We choose SNRs because they do not suffer from significant intrinsic absorption that may contribute to the measured extinction. In addition, owing to the large number of observed sources and the high quality data from the latest generation of X-ray detectors, we will be able to address which of the above factors contribute to the variations in the  $A_{\text{V}} - N_{\text{H}}$  relation found in the previous studies.

In Section 2 we summarize the methods used for the measurement of the hydrogen column density and optical extinction and present results towards 21 supernova remnants. In Section 3, we report the resulting  $A_{\text{V}} - N_{\text{H}}$  relation

**Table 1.** Optical extinction and X-ray measured hydrogen column densities as collected from literature.

SNR Name	$N_H$ ( $10^{22} \text{ cm}^{-2}$ )	Model <sup>1</sup>	Ref.	E(B−V) mag.	$A_V$ mag.	Method	Ref.
SNR G0.0+0.0	$14.7 \pm 1.2$	TP	(1)	$9.355 \pm 0.645$	$29 \pm 2$	NS	(2)
SNR G004.5+06.8	0.52	SE	(3)	$0.806 \pm 0.29$	$2.5 \pm 0.9$	FeII Ratio	(4)
SNR G6.5−0.1	$0.47 \pm 0.1$	TP	(5)	$1.15 \pm 0.15$	$3.57 \pm 0.47$	$H_\alpha/H_\beta$	(6)
SNR G13.3−1.3	$0.55 \pm 0.45$	TP	(7)	0.15	0.47	$H_\alpha/H_\beta$	(7)
SNR G53.6−2.2	$0.78 \pm 0.4$	TP	(8)	$1.15 \pm 0.15$	$3.57 \pm 0.47$	$H_\alpha/H_\beta$	(6)
SNR G54.1+0.3	$1.6 \pm 0.1$	PL	(9)	$2.581 \pm 0.226$	$8.0 \pm 0.70$	NS	(10)
SNR G67.7+1.8	$0.515 \pm 0.195$	TP	(11)	$1.7 \pm 0.3$	$5.27 \pm 0.93$	$H_\alpha/H_\beta$	(12)
SNR G69.0+2.7	$0.3 \pm 0.1$	PL	(13)	0.8	2.48	$H_\alpha/H_\beta$	(14)
SNR G74.0−8.5	$0.023 \pm 0.01$	TP	(15)	0.08	0.25	NS	(16)
SNR G109.1−1.0	$1.12 \pm 0.3$	AE	(17)	$0.995 \pm 0.205$	$3.15 \pm 0.65$	$H_\alpha/H_\beta$	(18)
SNR G111.7−02.1	$1.25 \pm 0.03$	BB	(19)	$1.613 \pm 0.129$	$5.0 \pm 0.40$	SII ratio	(20)
SNR G116.9+0.2	$0.79 \pm 0.12$	TP	(21)	$0.871 \pm 0.161$	$2.70 \pm 0.5$	$H_\alpha/H_\beta$	(22)
SNR G119.5+10.2	$0.28 \pm 0.05$	TP+PL	(23)	$0.410 \pm 0.132$	$1.27 \pm 0.41$	Extinction map	(24)
SNR G120.1+1.4	$0.435 \pm 0.045$	TP	(25)	$0.6 \pm 0.039$	$1.86 \pm 0.12$	NS	(26)
SNR G130.7+3.1	$0.416 \pm 0.08$	TP+PL	(27)	0.68	2.11	$H_\alpha/H_\beta$	(28)
SNR G132.7+1.3	$0.43 \pm 0.25$	TP	(5)	$0.710 \pm 0.040$	$2.201 \pm 0.124$	$H_\alpha/H_\beta$	(29)
SNR G184.6−5.8	$0.36 \pm 0.004$	PL	(30)	$0.50 \pm 0.060$	$1.55 \pm 0.186$	Ly $\alpha$ Absorption	(31)
SNR G260.4−3.4	$0.454 \pm 0.049$	2BB	(32)	0.839	2.60	NS	(33)
SNR G263.9−3.3	$0.0259 \pm 0.0001$	2BB	(34)	0.074	0.38	$H_\alpha/H_\beta$	(35)
SNR G296.5+10.0	$0.1 \pm 0.01$	2BB	(36)	0.161	0.50	$H_\alpha/H_\beta$	(37)
SNR G327.6+14.6	$0.07 \pm 0.01$	SI	(38)	0.11	0.34	HI/GC	(39)
SNR G332.4−00.4	$0.7 \pm 0.2$	2BB	(40)	$1.516 \pm 0.29$	$4.70 \pm 0.90$	FeII Ratio	(4)

<sup>1</sup> Model abbreviations: TP: Thermal Plasma, PL: Power-Law, BB: Blackbody, AE: Absorption Edge modeling, NS: Nearby Stars, SE: Synchrotron Emission, SI: Shocked ISM

References : (1) Sakano et al. (2004); (2) Predehl & Truemper (1994); (3) Reynolds et al. (2007); (4) Oliva et al. (1989); (5) Rho & Petre (1998); (6) Long et al. (1991); (7) Seward et al. (1995); (8) Saken et al. (1995); (9) Lu et al. (2002); (10) Koo et al. (2008); (11) Hui & Becker (2008); (12) Mavromatakis et al. (2001); (13) Li et al. (2005); (14) Hester & Kulkarni (1989); (15) Katsuda et al. (2008); (16) Parker (1967); (17) Durant & van Kerkwijk (2006); (18) Fesen & Hurford (1995); (19) Hwang et al. (2004); (20) Hurford & Fesen (1996); (21) Craig et al. (1997); (22) Fesen et al. (1997); (23) Slane et al. (1997); (24) Mavromatakis et al. (2000); (25) Warren et al. (2005); (26) Ruiz-Lapuente (2004); (27) Gotthelf et al. (2007); (28) Fesen et al. (1988); (29) Fesen et al. (1995); (30) Massaro et al. (2006); (31) Sollerman et al. (2000); (32) Hui & Becker (2006); (33) Gorenstein (1975); (34) Manzali et al. (2007); (35) Manchester et al. (1978); (36) De Luca et al. (2004); (37) Ruiz (1983); (38) Acero et al. (2007); (39) Raymond et al. (1995); (40) De Luca et al. (2006).

and discuss any systematic uncertainties that may affect this result.

## 2 EXTINCTION AND X-RAY ABSORPTION MEASUREMENTS

Of the 243 supernova remnants included in the extensive catalog of Guseinov et al. (2003, 2004a,b), approximately 143 sources have been observed with the *Chandra*, *XMM-Newton*, or *Suzaku* satellites. The high quality spectral data obtained with these satellites allowed for a more precise measurement of the hydrogen column density by modeling both the X-ray continuum and the line features in the source spectra. We compiled the hydrogen column density measurements for these 143 sources (see Table 1 for the relevant references).

We then searched for independent measurements of the optical extinction towards all the SNRs listed in the Guseinov et al. (2003, 2004a,b) catalog. Unlike the case of X-ray extinction, our search revealed that there is a lack of reported measurements of optical extinction or reddening: Out of the 243 SNRs, we were able to obtain only 22 independent  $A_V$  measurements. Luckily, this set of 22 sources is

a subset of the 143 sources, for which we have high-resolution measurements of the X-ray extinction with the new X-ray satellites.

We discuss here the data as well as the methods that are used to determine the hydrogen column density and optical extinction. This will be important in quantifying systematic uncertainties in the correlation between optical and X-ray extinction.

### 2.1 X-ray Hydrogen Column Density Measurements

Hydrogen column density measurements of supernova remnants in the X-rays are performed by modeling their spectra, usually in the 0.2 – 8.0 keV range. Extinction is determined by comparing an intrinsic source spectrum, such as a blackbody, a power-law, or a thermal plasma emitting bremsstrahlung radiation, with the observed spectrum. The model parameters inferred from spectral fits are often correlated with the hydrogen column density, especially when the analyzed data cover a small range in the X-ray band and the energy resolution is low (see, e.g., Figure 2 of Predehl & Schmitt 1995). Moreover, when the spectra of

extended sources are observed with detectors of low angular resolution, the intrinsic variations of the source spectra that cannot be resolved bias the results.

Observations with the Chandra, XMM-Newton, and Suzaku satellites (see, e.g., Paerels & Kahn 2003; Juett et al. 2004; Juett et al. 2006) yield significant improvements in both of these areas. The increased angular resolution of the telescopes make it possible to model small regions within the SNR and detect local changes in the intrinsic spectral properties. At the same time, the increased energy resolution and signal to noise ratios lead to better modeling of both the continuum spectra and of line features. In the most favorable cases, e.g., SNR G109.1–1.0, X-ray absorption edges of heavier elements, such as Mg and Ne, can be directly detected, completely eliminating the dependence of the column density on the assumed intrinsic X-ray spectrum of the source (Durant & van Kerkwijk 2006). All of these lead to better constrained hydrogen column densities compared to earlier studies.

In the majority of the SNRs in our study, the X-ray spectra were fit with a thermal plasma model, where emission lines were also taken into account whenever possible (see Table 1). The remaining spectra were modeled either by a power-law or a combination of two blackbodies. In order to make the analysis as free from the assumed continuum model as possible, we did not exclude from the study the reported hydrogen column density measurements where other continuum models were used.

For the spatially resolved SNRs, hydrogen column densities measured towards different regions of the remnant can show variations that are larger than the statistical errors of each measurement. In these cases, we adopted the average of these values with an error that accounts for the observed scatter. Finally, in the cases where the central point sources can be resolved, we also used the  $N_{\text{H}}$  measurement obtained by modeling the emission from the central neutron star surface either by a blackbody, a power-law, or a hydrogen atmosphere model.

## 2.2 Optical Extinction Measurements

Determining the optical extinction towards SNRs is more challenging than the hydrogen column density measurements in the X-rays and demands high signal to noise ratio spectra. Nearly all of the methods involve measuring the reddening using the intensity ratio of two emission lines and converting the reddening into an optical extinction.

One of the well known and reliable methods of measuring the extinction is based on the Balmer decrement, which involves the intensity ratio of the observed  $H_{\alpha}$  (6563 Å) and  $H_{\beta}$  (4861 Å) emission lines. The observed relative intensity is compared to that expected for a gaseous nebula with typical temperature and electron density. Since this ratio depends very weakly on the physical conditions of the nebula, the theoretical ratio can be calculated with minimal uncertainty. Thus, the comparison allows a measurement of the reddening, and hence, of the optical extinction (see, e.g., Osterbrock 1989; Lequeux 2005). The majority of the optical extinction measurements presented here are found using this method since both of the lines lie in the optical range and, in most cases, are strong enough to be resolved.

One other frequently used method involves measur-

ing the SII multiplet ratios (Miller 1968) in the infrared ( $\sim 10320$  Å) and blue ( $\sim 4068$  Å). As with the Balmer decrement method, this ratio also depends only very weakly on the temperature and density in the remnant. However, the disadvantage of this method is the fact that it is not always practical to perform spectral observations in both of these wavelength regions with high enough spectral resolution.

In a third method, the two most prominent IR transitions of Fe[II] (1.6435  $\mu\text{m}$  and 1.2567  $\mu\text{m}$ ) that arise from the same upper level can be used. Their intensity ratio does not depend strongly on the temperature and density of the gas (Oliva et al. 1989), allowing for a determination of the extinction. In our sample, the optical extinction towards SNR G332.4-00.4 and SNR G004.5+06.8 has been measured with this method by (Oliva et al. 1989), using a theoretical ratio of 1.36 for these lines (Nussbaumer & Storey 1988).

A final method involves using nearby stars with known distances to estimate the extinction towards the SNR. In Table 1, we denoted the four optical extinction measurements obtained with this method as “nearby stars”.

In Table 1 we present the compilation of the optical extinction data. For the cases where only the reddening  $E(B-V)$  measurement was reported, we converted these to an extinction ( $A_V$ ) assuming a  $A_V = 3.1E(B-V)$  relation (see, e.g., Fitzpatrick 2004; Savage & Mathis 1979). Finally, in the absence of any reported systematic or statistical errors, we assigned a 15% uncertainty on the measurements for the purposes of the fit only, which is similar to the average errors given for the other measurements. These cases are left without errors in Table 1.

## 3 RESULTS AND DISCUSSION

We plot in Figure 1 the optical extinction,  $A_V$ , for 22 supernova remnants against their hydrogen column density, measured from their high energy resolution X-ray spectra. Figure 1 includes a typical 15% error on the optical extinction for those remnants that did not have reported errors on this measurement (see Table 1). We performed a linear fit between these quantities and obtained the best-fit relation

$$N_{\text{H}}(\text{cm}^{-2}) = (2.21 \pm 0.09) \times 10^{21} A_V, \quad (1)$$

where the errors correspond to 1- $\sigma$  statistical uncertainty. We present the best-fit line in Figure 1. This relation can also be expressed as  $N_{\text{H}}(\text{cm}^{-2}) = (6.86 \pm 0.27) \times 10^{21} E(B-V)(\text{mag})$  between the reddening and the hydrogen column density.

We then investigated whether the continuum models that are used to fit the X-ray observations to measure the hydrogen column density affect the results found for the  $A_V - N_{\text{H}}$  relation. Specifically, we looked into the power-law continuum models, which are known to give higher values for the hydrogen column density than others. To this end, we compared the  $A_V - N_{\text{H}}$  relation that we found from fitting the entire sample to that derived when the three power-law continuum fits in the sample were excluded. We found that the resulting relations do not differ significantly from each other either in the slope or in the errors. Specifically, excluding the subset of observations where the X-ray continuum was modeled with a power-law results in the relation

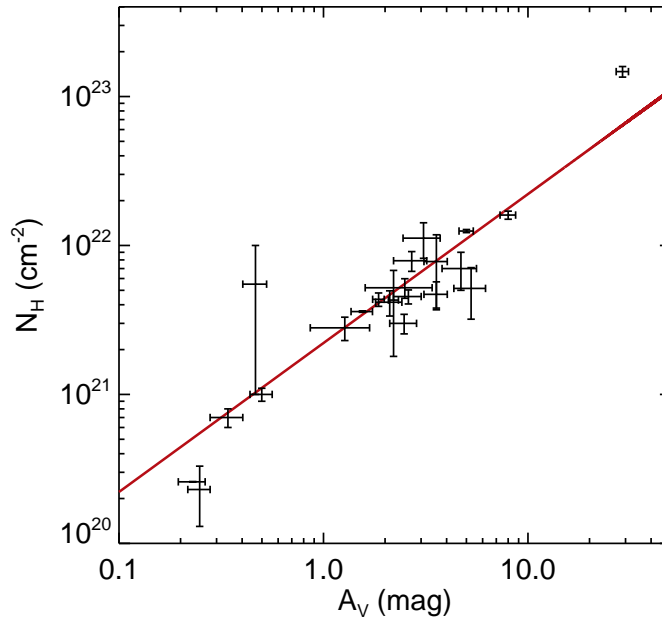


**Figure 1.** The observed correlation between hydrogen column density and optical extinction, together with the best fit linear model, found as  $N_{\text{H}} = (2.21 \pm 0.09) \times 10^{21} \times A_{\text{V}}$ .

$N_{\text{H}} = (2.29 \pm 0.11) \times 10^{21} \times A_{\text{V}}$ , while all the data yield  $N_{\text{H}} = (2.21 \pm 0.09) \times 10^{21} \times A_{\text{V}}$ .

Another possible systematic uncertainty is introduced by the use of solar abundances when measuring the hydrogen column density from X-ray spectra. It has been shown that different assumptions on the elemental abundances (e.g., solar vs. ISM) in the interstellar medium can lead to  $\sim 5\%$  variation in the hydrogen column density (Wilms et al. 2000). The  $N_{\text{H}}$  values used in our study could be subject to similar systematic uncertainties.

Comparing our result with previous studies, we find that it is in very good agreement with the relation given by Gorenstein (1975)  $N_{\text{H}}(\text{cm}^{-2}) = (2.22 \pm 0.14) \times 10^{21} A_{\text{V}}$ , while it differs at the  $3\sigma$  level from the result obtained by Predehl & Schmitt (1995)  $N_{\text{H}}(\text{cm}^{-2}) = (1.79 \pm 0.03) \times 10^{21} A_{\text{V}}$ . This difference can be attributed to a number of causes: ROSAT’s narrow bandpass, which does not allow tight constraints on the intrinsic spectral shape; the authors’ assumption that the intrinsic spectra of all their sources are power laws; possible intrinsic absorption; and the uncertain properties of the optical counterparts, which affect the assumed extinction values.

Despite the improvements on the number and quality of the observations, there may still be a number of systematic errors and selection effects present in our study. A larger, homogeneous sample of supernova remnants, studied with both the last generation X-ray satellites as well as with sensitive optical spectrographs will help refine the studies of the interstellar medium and the relation between the optical extinction and the hydrogen column density in the Galaxy, hence the dust to gas ratio. Increasing the number of sources in the sample may also allow for a search for variations in the relation towards different lines of sight.

## ACKNOWLEDGMENTS

We would like to thank the anonymous referee for very useful comments. This work was supported by NSF grant AST 07-08640.

## REFERENCES

- Acero F., Ballet J., Decourchelle A., 2007, *A&A*, 475, 883
- Craig W. W., Hailey C. J., Pisarski R. L., 1997, *ApJ*, 488, 307
- De Luca A., Caraveo P. A., Mereghetti S., Tiengo A., Bignami G. F., 2006, *Science*, 313, 814
- De Luca A., Mereghetti S., Caraveo P. A., Moroni M., Mignani R. P., Bignami G. F., 2004, *A&A*, 418, 625
- Durant M., van Kerkwijk M., 2006, *ApJ*, 650, 1082
- Fesen R. A., Downes R. A., Wallace D., Normandeau M., 1995, *AJ*, 110, 2876
- Fesen R. A., Hurford A. P., 1995, *AJ*, 110, 747
- Fesen R. A., Kirshner R. P., Becker R. H., 1988, in Roger R. S., Landecker T. L., eds, *IAU Colloq. 101: Supernova Remnants and the Interstellar Medium 3C58’S Filamentary Radial Velocities, Line Intensities, and Proper Motions*. p. 55
- Fesen R. A., Winkler F., Rathore Y., Downes R. A., Wallace D., 1997, *AJ*, 113, 767
- Fitzpatrick E. L., 2004, in Witt A. N., Clayton G. C., Draine B. T., eds, *Astrophysics of Dust Vol. 309 of Astronomical Society of the Pacific Conference Series, Interstellar Extinction in the Milky Way Galaxy*. pp 33–+
- Gorenstein P., 1975, *ApJ*, 198, 95
- Gotthelf E. V., Helfand D. J., Newburgh L., 2007, *ApJ*, 654, 267

- Guseinov O. H., Ankay A., Tagieva S. O., 2003, *SerAJ*, 167, 93
- Guseinov O. H., Ankay A., Tagieva S. O., 2004a, *SerAJ*, 169, 65
- Guseinov O. H., Ankay A., Tagieva S. O., 2004b, *SerAJ*, 168, 55
- Hester J. J., Kulkarni S. R., 1989, *ApJ*, 340, 362
- Hui C. Y., Becker W., 2006, *A&A*, 454, 543
- Hui C. Y., Becker W., 2008, arXiv:0812.2186v1 [astro-ph]
- Hurford A. P., Fesen R. A., 1996, *ApJ*, 469, 246
- Hwang U., Laming J. M., Badenes C., Berendse F., Blondin J., Cioffi D., DeLaney T., Dewey D., Fesen R., Flanagan K. A., Fryer C. L., Ghavamian P., Hughes J. P. e. a., 2004, *ApJL*, 615, L117
- Juett A., Schulz N., Chakrabarty D., 2004, *ApJ*, 612, 308
- Juett A. M., Schulz N. S., Chakrabarty D., Gorczyca T. W., 2006, *ApJ*, 648, 1066
- Katsuda S., Tsunemi H., Uchida H., Miyata E., Nemes N., Miller E. D., Mori K., Hughes J. P., 2008, *PASJ*, 60, 115
- Koo B. C., McKee C. F., Lee J. J., Lee H. G., Lee J. E., Moon D. S., Hong S. S., Kaneda H., Onaka T., 2008, *ApJL*, 673, L147
- Lequeux J., 2005, *The interstellar medium. The interstellar medium*, EDP Sciences, Springer, Berlin, 2005
- Li X. H., Lu F. J., Li T. P., 2005, *ApJ*, 628, 931
- Long K. S., Blair W. P., Matsui Y., White R. L., 1991, *ApJ*, 373, 567
- Lu F. J., Wang Q. D., Aschenbach B., Durouchoux P., Song L. M., 2002, *ApJL*, 568, L49
- Manchester R. N., Lyne A. G., Goss W. M., Smith F. G., Disney M. J., Hartley K. F., Jones D. H. P., Wellgate G. B., Danziger I. J., Murdin P. G., Peterson B. A., Wallace P. T., 1978, *MNRAS*, 184, 159
- Manzali A., De Luca A., Caraveo P. A., 2007, *ApJ*, 669, 570
- Massaro E., Campana R., Cusumano G., Mineo T., 2006, *A&A*, 459, 859
- Mavromataki F., Papamastorakis J., Paleologou E. V., Ventura J., 2000, *A&A*, 353, 371
- Mavromataki F., Papamastorakis J., Ventura J., Becker W., Paleologou E. V., Schaudel D., 2001, *A&A*, 370, 265
- Miller J. S., 1968, *ApJL*, 154, L57
- Nussbaumer H., Storey P. J., 1988, *A&A*, 193, 327
- Oliva E., Moorwood A. F. M., Danziger I. J., 1989, *A&A*, 214, 307
- Osterbrock D. E., 1989, *Astrophysics of gaseous nebulae and active galactic nuclei*. University Science Books, CA, 1989, 422 p.
- Paerels F. B. S., Kahn S. M., 2003, *ARA&A*, 41, 291
- Parker R. A. R., 1967, *ApJ*, 149, 363
- Predehl P., Schmitt J. H. M. M., 1995, *A&A*, 293, 889
- Predehl P., Truemper J., 1994, *A&A*, 290, L29
- Raymond J. C., Blair W. P., Long K. S., 1995, *ApJL*, 454, L31
- Reina C., Tarengi M., 1973, *A&A*, 26, 257
- Reynolds S. P., Borkowski K. J., Hwang U., Hughes J. P., Badenes C., Laming J. M., Blondin J. M., 2007, *ApJL*, 668, L135
- Rho J., Petre R., 1998, *ApJL*, 503, L167
- Ruiz M. T., 1983, *AJ*, 88, 1210
- Ruiz-Lapuente P., 2004, *ApJ*, 612, 357
- Sakano M., Warwick R. S., Decourchelle A., Predehl P., 2004, *MNRAS*, 350, 129
- Saken J. M., Long K. S., Blair W. P., Winkler P. F., 1995, *ApJ*, 443, 231
- Savage B. D., Mathis J. S., 1979, *ARA&A*, 17, 73
- Seward F. D., Dame T. M., Fesen R. A., Aschenbach B., 1995, *ApJ*, 449, 681
- Slane P., Seward F. D., Bandiera R., Torii K., Tsunemi H., 1997, *ApJ*, 485, 221
- Sollerman J., Lundqvist P., Lindler D., Chevalier R. A., Fransson C., Gull T. R., Pun C. S. J., Sonneborn G., 2000, *ApJ*, 537, 861
- Warren J. S., Hughes J. P., Badenes C., Ghavamian P., McKee C. F., Moffett D., Plucinsky P. P., Rakowski C., Reynoso E., Slane P., 2005, *ApJ*, 634, 376
- Wilms J., Allen A., McCray R., 2000, *ApJ*, 542, 914